nature physics

LETTERS

PUBLISHED ONLINE: 19 SEPTEMBER 2010 | DOI: 10.1038/NPHYS1762

Observation of topological order in a superconducting doped topological insulator

L. Andrew Wray[1,2,3], Su-Yang Xu[1], Yuqi Xia[1], Yew San Hor[4], Dong Qian[1], Alexei V. Fedorov[3], Hsin Lin[5], Arun Bansil[5], Robert J. Cava[4] and M. Zahid Hasan[1,3,6]*

Experimental observation of topological order in three-dimensional bulk solids has recently led to a flurry of research activity[1–21]. Unlike the two-dimensional electron gas or quantum Hall systems, three-dimensional topological insulators can harbour superconductivity and magnetism, making it possible to study the interplay between topologically ordered phases and broken-symmetry states. One outcome of this interplay is the possible realization of Majorana fermions—quasiparticles that are their own antiparticles—on topological surfaces, which is of great interest in fundamental physics[9–13,22–24]. Here we present measurements of the bulk and surface electron dynamics in Bi_2Se_3 doped with copper with a transition temperature T_c up to 3.8 K, observing its topological character for the first time. Our data show that superconductivity occurs in a bulk relativistic quasiparticle regime where an unusual doping mechanism causes the spin-polarized topological surface states to remain well preserved at the Fermi level of the superconductor where Cooper pairing takes place. These results suggest that the electron dynamics in superconducting Bi_2Se_3 are suitable for trapping non-Abelian Majorana fermions. Details of our observations constitute important clues for developing a general theory of topological superconductivity in doped topological insulators.

Topological insulators embody a new state of quantum matter characterized by the topological invariants or order of the bulk electronic structure rather than a spontaneously broken symmetry of the underlying electron systems[1–8]. Recent observations of superconductivity in the doped topological insulators Bi_2Se_3 and Bi_2Te_3 led to speculations that these compounds may provide platforms for studying the interplay between topological and broken-symmetry order[22–24]. Theoretically, superconducting pairing induced on a two-dimensional topological surface state through proximity to a bulk superconductor is believed to be inherently unconventional, with the potential to host non-Abelian (non-commutative) particles such as Majorana fermions in their vortices[12,13,20]. The quasiparticle excitations in such superconductors also defy traditional classification as a singlet or triplet form of the Cooper pairing state[20]. To ensure that a superconducting material is capable of hosting such two-dimensional vortices in their superconducting states, the spin-polarized surface states must be non-degenerate with the bulk bands where Cooper pairing takes place, ideally, at temperatures larger than 1 K.

It has recently been found that 10% copper is needed to bring about superconductivity in bulk Bi_2Se_3, with a relatively large transition temperature of $T_C = 3.8$ K confirmed by the observation of the Meissner effect[22]. However, all known measured band structures as well as band calculations of undoped Bi_2Se_3 so far suggest that the topological surface states cannot remain non-degenerate at the Fermi level under the carrier doping that is required to induce superconductivity with relatively large $T_C = 3.8$ K. Therefore, it has long been expected that the topological effects on the surface of $Cu_xBi_2Se_3$ would be washed out at the superconducting compositions (Supplementary Information) and such a system cannot be a platform for Majorana fermions. In this work, we experimentally investigate these issues with angle-resolved photoemission spectroscopy (ARPES).

We have systematically investigated doping-induced changes in the electronic ground state by examining several stoichiometric crystals with copper added ($Cu_xBi_2Se_3$, $x = 0$, 0.01, 0.05, 0.12) and contrasted these doping levels with a case in which copper is substituted for bismuth as $Cu_{0.1}Bi_{1.9}Se_3$. Our results, summarized in Fig. 1, suggest that copper atoms can add holes or electrons depending on their net preference for occupying different kinds of site in the Bi_2Se_3 lattice. Copper atoms intercalated between van der Waals-like bonded selenium planes (Cu_{int}) in the crystal are known to be single electron donors, whereas substitutional defects in which copper replaces bismuth in the lattice (Cu_{Bi}) contribute two holes to the system, which is similar to the behaviour reported in the impurity-atom study on the Bi_2Se_3 matrix[25]. The qualitative result of copper addition is a gradual enlargement of the Fermi surface from electron doping and, further surprisingly, a strong reduction in surface electron velocities through reshaping of the surface conduction band. The slope of the surface-state band represents particle velocity, and is globally reduced in amplitude by 30% above the Dirac point when copper doping of $x = 0.05$ is added to the stoichiometric compound (see Fig. 2c). Assuming that the surface-state Dirac point energy is fixed relative to bulk bands, reducing the slope of the surface state increases separation between the bulk and surface conduction bands, a characteristic that increases the stability of the topological surface state and is of great importance for stabilizing the topological nature of superconductivity. This effect acts together with the nonlinear doping mechanism reported here to preserve the two-dimensional topological surface state at superconducting doping. Therefore, our experimental results, in contrast to first-principle calculations, suggest that the crystal surface of $Cu_xBi_2Se_3$ can, in fact, host two-dimensional vortices, which is critical for observing the non-Abelian statistics of the vortex Majorana fermions on the topological surface.

[1]Joseph Henry Laboratories, Department of Physics, Princeton University, Princeton, New Jersey 08544, USA, [2]Princeton Center for Complex Materials, Princeton University, Princeton, New Jersey 08544, USA, [3]Advanced Light Source, Lawrence Berkeley National Laboratory, Berkeley, California 94305, USA, [4]Department of Chemistry, Princeton University, Princeton, New Jersey 08544, USA, [5]Department of Physics, Northeastern University, Boston, Massachusetts 02115, USA, [6]Princeton Institute for Science and Technology of Materials, Princeton University, Princeton, New Jersey 08544, USA.
*e-mail: mzhasan@Princeton.edu.

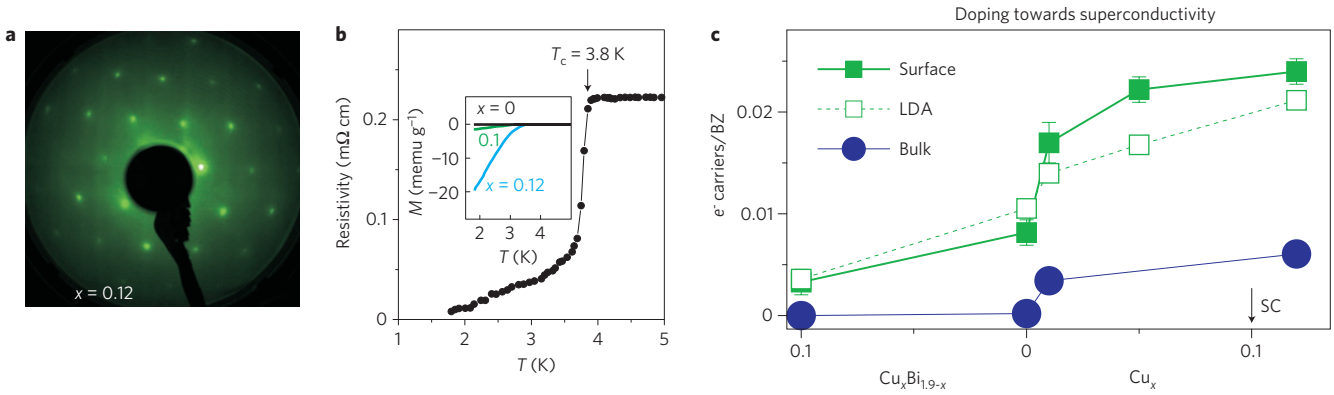

Figure 1 | Superconductivity in $Cu_xBi_2Se_3$ crystals. a, A low-energy electron diffraction image taken at 200 eV electron energy provides evidence for a well-ordered surface with no sign of superstructure modulation. **b**, Resistivity and magnetic susceptibility measurements for samples used in this study. Samples exhibit a superconducting transition at 3.8 K at optimal copper doping ($x = 0.12$). **c**, The number of charge carriers is calculated from the Luttinger count (Fermi surface area/Brillouin zone (BZ) area, ×2 for the doubly degenerate bulk band). Local density approximation (LDA) predictions show the carrier density obtained by aligning the local-density-approximation band structure with the experimentally determined binding energy of the Dirac point.

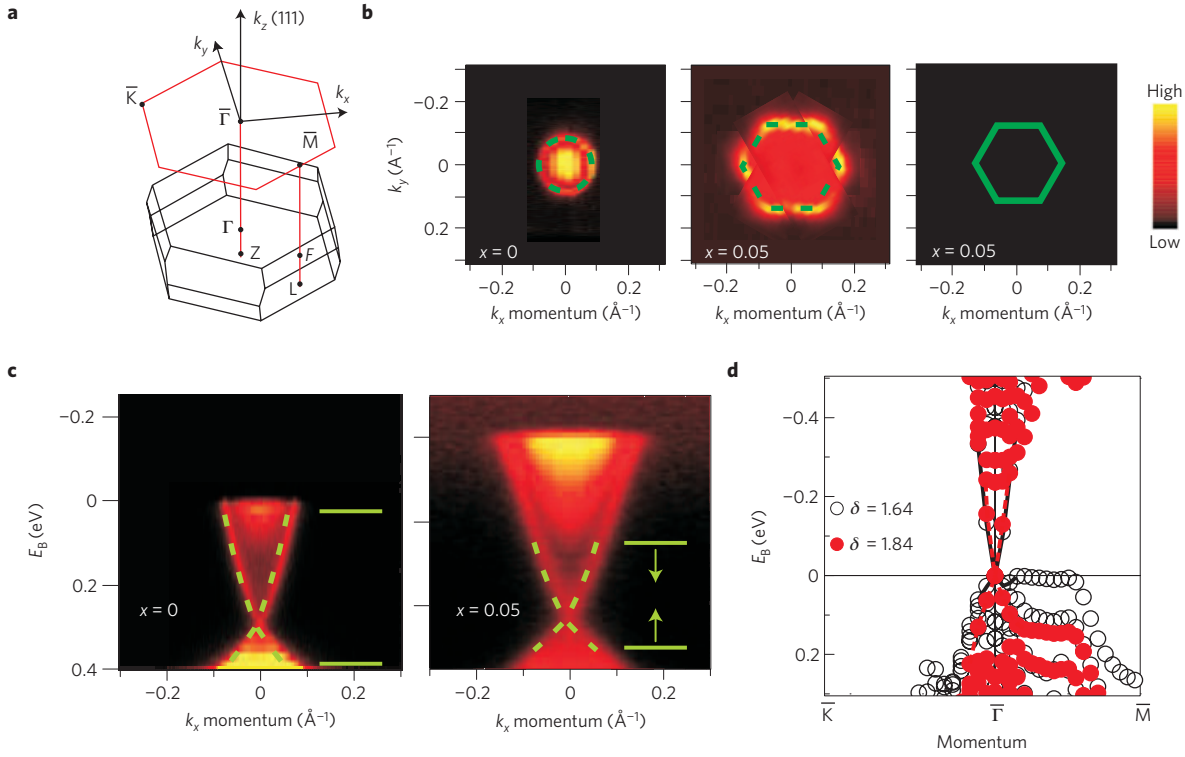

Figure 2 | Surface electron kinematics of $Cu_xBi_2Se_3$. a, The hexagonal surface Brillouin zone of $Cu_xBi_2Se_3$ shown above a diagram of the three-dimensional bulk Brillouin zone. **b**, Symmetrized surface-state Fermi surfaces, with (right) a generalized gradient approximation prediction based on the experimental Fermi level. **c**, Photoemission measurements at high photon energy ($E > 20$ eV) for non-superconducting $Cu_xBi_2Se_3$, demonstrating a reduced surface-state dispersion after copper is added. **d**, When the Bi–Se plane spacing at the surface of a 12-layer slab is increased by 0.2 Å (1.64–1.84 Å), dispersion in the upper Dirac cone increases by 16%. Binding energy scales have been rigidly shifted in **c** and **d** to align the Dirac points.

The addition of copper causes the surface-state kinetics to become strongly hexagonally anisotropic (Fig. 2b), a deformation that makes the surface susceptible to spin-fluctuation or magnetic instabilities[21]. This is due to the fact that the topological surface states in Bi_2Se_3 are spin polarized[8]. The carrier density in the surface state is much greater than the density in the bulk, as estimated by the Luttinger count applied to the photoemission data (Fig. 1c), suggesting that the surface carries a screened negative charge within the normal state of the superconductor. We also observed that attempting to force the creation of Cu_{Bi} replacement defects by adding less bismuth results in very weak hole doping for $Cu_{0.1}Bi_{1.9}Se_3$ (Fig. 1c), raising the bulk conduction band entirely above the Fermi level. On doping into the superconducting regime ($x = 0.12$), the Fermi energy is found to be raised to 0.25 eV above the bulk conduction-band minimum, placing the Fermi level in the linear (relativistic) regime of bulk band dispersion. Contrasting the bulk band line shape with classical and relativistic Dirac-like energy dispersions with the same mass ($M = 0.155M_e$) reveals that electron kinetics begin to enter the linear relativistic regime within ~0.1 eV of the Fermi level (Fig. 3f). A slight bend in the dispersion centred near 90 meV binding energy (E_B; Fig. 3f inset) may suggest electron–boson interactions in

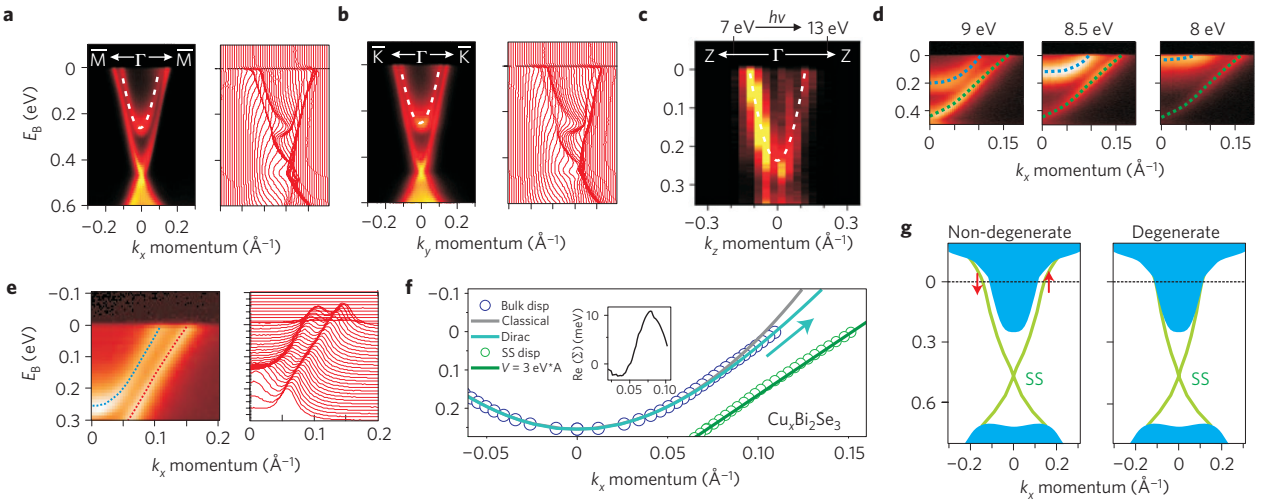

Figure 3 | Band topology at the superconducting composition. a,**b**, Momentum dependence of the bulk and surface conduction bands in superconducting $Cu_{0.12}Bi_2Se_3$ measured with low-energy (9.75 eV) photons for enhanced bulk sensitivity. **c**, Dispersion along the *z* axis, examined by varying incident photon energy. **d**, Bulk and surface bands remain separate at intermediate k_z values. **e**,**f**, Energy of the bulk electrons compared with Dirac ($v_C = 6$ eV Å) and classical (parabolic) fits with a mass of $0.155M_e$. Surface-state (SS) dispersion is also plotted. Inset: Self-energy with respect to the Dirac fit. **g**, The surface electronic structure presents a non-trivial topological setting for superconductivity because (green) surface and (blue) bulk bands do not overlap.

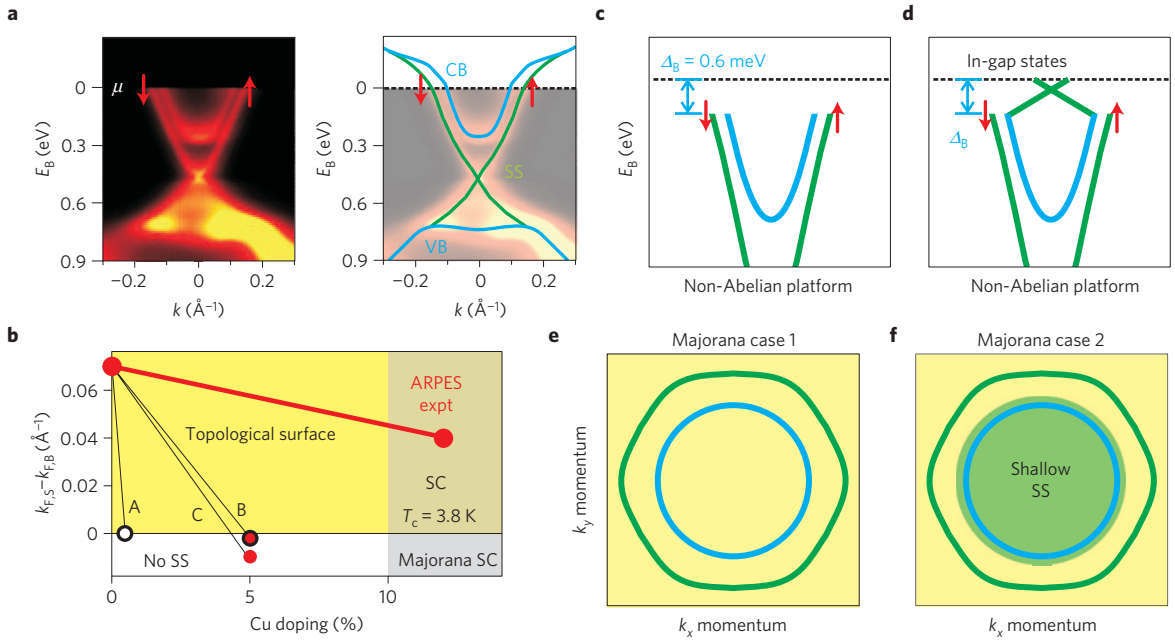

Figure 4 | Superconducting symmetry breaking on the topological surface. a, Bulk and surface electrons are non-degenerate at the Fermi level. VB, valence band; CB, conduction band. **b**, A phase diagram compares (expt) the measured superconducting topology with preliminary expectations based on cases in which (A) each Cu atom donates one doped electron, (B) the experimental chemical potential is applied to generalized-gradient-approximation band structure and (C) the experimental chemical potential is applied to the band structure of undoped Bi_2Se_3. **c**–**f**, Electronic states expected below T_C for even-parity superconductivity (**c**,**e**) and an example of odd-parity 'topological superconductivity' (**d**,**f**). **e** and **f** show states within 5 meV of the Fermi level. Both cases allow the superconducting state to host non-Abelian particles such as Majorana fermions.

the system, also ubiquitously observed in other superconducting materials. Therefore, Cooper pairing in the superconducting state takes place in this relativistic regime where the chemical potential lies. A three-dimensional massive Dirac-like dispersion in topological spin–orbit materials is expected as a direct result of the band-inversion mechanism that causes the topological insulator state, and has also been experimentally observed in other topological insulator $Bi_{1-x}Sb_x$ alloys[4]. In $Cu_xBi_2Se_3$, calculations predict that band inversion occurs at the Γ-point ($k_x = k_y = k_z = 0$) in the centre of the bulk conduction band, leading to a spin–orbit-induced Dirac-like bulk band, in qualitative agreement with our experiments.

Several features of this unusual spin–orbit band structure provide critical insights into characteristics of the superconducting condensate wavefunction. Bulk Fermi momenta of 0.110 ± 3 Å^{-1} and 0.106 ± 3 Å^{-1} are observed along the $\overline{\Gamma}$–$\overline{M}$ and $\overline{\Gamma}$–$\overline{K}$ directions respectively. Varying the incident energy to observe dispersion along the $\hat{z}$ axis (Γ–Z direction) reveals a Fermi momentum of 0.12 ± 1 Å^{-1}, suggesting that the bulk electron kinetics are three-dimensionally isotropic. Carefully tracing the band (Fig. 3e,f)

reveals a Fermi velocity of 3.5 ± 2 eV Å along $\overline{\Gamma}$–$\overline{M}$ and 4.1 ± 2 eV Å along $\overline{\Gamma}$–$\overline{K}$, estimated within 50 meV of the Fermi level. The gap between bulk valence and conduction bands appears to be unchanged on copper doping. In a material-specific band-structure-based modelling of superconductivity, considering a competition between inter-site and intra-site orbital coupling, suggests that the superconducting pairing symmetry in this system is partially determined by the ratio between the Dirac rest mass and the doped chemical potential[20] ('μ'), when the conduction band is fitted to a relativistic Hamiltonian of the form:

$$H_0(k) = M^*\Gamma_0 + v_C^*(k_x\Gamma_1 + k_y\Gamma_2 + k_z\Gamma_3) \quad (1)$$

where M^* is the rest mass, v_C is the velocity of the three-dimensional Dirac band and the Γ_i terms ($i = 0; \ldots; 3$) are the 4×4 Dirac Gamma matrices. For this discussion, we assume that v_C is isotropic to illustrate the essential points, although our data show some further details that it may be smaller in the z-axis direction. The chemical potential of this Hamiltonian is equal to the sum of the rest mass and the binding energy of the valence-band minimum, which can be experimentally evaluated from our photoemission data. In an ideal Dirac band structure, the rest mass will be equal to half the band gap, or 150 meV (giving $M^* = 0.15$ eV, $\mu = 0.15$ eV $+ 0.25$ eV, and $M^*/\mu \sim 1/3$). Owing to asymmetries between conduction- and valence-band dispersion in the real experimental system, a larger effective rest mass is used to fit the curvature of the bottom of the conduction band in Fig. 3f, consistent with a ratio of $M^*/\mu = 3/4$. These ratios are small enough to allow the theoretical possibility that the bulk superconducting wavefunction may have an odd (-1) parity symmetry value[20]. A dispersion anomaly that we have noted in the inset to Fig. 3f also affects low-energy electron kinetics, making the bands more linear locally at the Fermi level. Dispersion anomalies, often referred to as 'kinks' in photoemission literature, are a common property of band structure in real superconducting materials[26]. The presence of the kink depresses the value of m/μ in the favourable direction for realizing odd-parity pairing proposed in ref. 20.

The observed spin–orbit band topology in our data fixes several key parameters related to the superconductivity. The superconducting coherence length can be estimated from the average Fermi velocity we observe here to be about 2,000 Å ($\xi_0 \sim 0.2 \times \hbar v_F / K_B T_C = 0.2 \times 3.8$ eVÅ$/(K_B \times 3.8\,\mathrm{K}) = 2{,}000$ Å), assuming minimal scattering and a superconducting gap related to T_C by the Bardeen–Cooper–Schrieffer formula. This value is about 1–2 orders of magnitude greater than that seen in the cuprates ($\xi_0 \sim 100$–200 Å) or cobaltates ($\xi_0 \sim 200$ Å; refs 26,27). The phase-ordering temperature scale, also estimated from our data, is approximately $T_\theta = 60{,}000$ K, four orders of magnitude larger than the superconducting critical temperature of 3.8 K ($T_\theta = \xi_0 \times \hbar^2 n_e / 2\,m^* = 2{,}000$ Å $\times\, \hbar^2 \times 10^{20}\ \mathrm{cm}^{-3}/(2 \times .155 M_e) = 60{,}000$ K). A large coherence length and high phase-ordering temperature suggest that key properties of the pairing state can be described within a mean-field picture. On the basis of this, we estimate the superconducting gap to be about $\sim$0.6 meV ($3.5 \times K_B T_C / 2 = 0.6$ meV).

The fact that superconductivity occurs in the relativistically linear bulk bands in $Cu_xBi_2Se_3$ as seen in our data allows unusual combinations of spin and orbital mixing in the bulk superconducting state, making pairing take an unusual form; more remarkably however, probing near the Fermi level, our data show that the spin-textured surface and doubly degenerate bulk bands are well separated by 0.04 Å^{-1} in momentum and by an energy spacing of about $\Delta_E = 130$ meV, establishing that bulk superconducting pairing occurs in the presence of a non-degenerate, spin-polarized two-dimensional topological surface state, and that theoretical constraints ensuring unconventional superconductivity induced in the topological surface band will define key properties of the pairing wavefunction[3,12,28].

Topological surface states are completely determined by the bulk band-structure topology[3,29], ensuring that superconducting symmetry breaking in the bulk bands must necessarily have a proximity effect on the surface spectrum. Three-dimensional topological insulators doped into a superconducting phase are classified by an integer invariant ('n'), rather than a Z_2 invariant (parity invariant; ref. 20). The specific band structure and strong spin–orbit coupling of $Cu_xBi_2Se_3$ suggest that the topological invariant 'n' may be non-zero, allowing the possibility of topological superconductivity in $Cu_xBi_2Se_3$. This is further supported by the fact that the ratio m/μ for $Cu_xBi_2Se_3$ is well into the topological regime[20] as seen in our data. The exact nature of the superconducting order parameter will depend on the parity of the pairing wavefunction, which may be even or odd under inversion because Bi_2Se_3 is a centrosymmetric crystal. Of the two remaining possibilities, even parity will result in a fully gapped band structure, and odd parity will generate new surface states resembling those shown in Fig. 4d (ref. 20). In either scenario, the preserved topological spin-polarized surface state will allow the superconducting wavefunction to host Majorana fermions that exhibit non-Abelian quantum statistics[12], which might be manipulated adiabatically if the surface is fully gapped (even parity, case 1 in Fig. 4). In the second, odd-parity case, the material will also be the first known realization of a new state of matter specifically termed a 'topological superconductor'[9,11,20]. Topological superconductors spontaneously realize a Majorana surface state. Although the exact determination of order-parameter phase (even or odd) will require low-temperature phase-sensitive measurements on ultrahigh-purity large single crystals, the unusual doping evolution and electron dynamics observed here constitute the key ingredients for developing a theory of spontaneous symmetry breaking and topological superconductivity in strongly spin–orbit coupled materials.

Methods

Experimental observation of surface and bulk separation and their microscopic electron kinetics involves several significant technical challenges. These are detailed in the Supplementary Information. ARPES measurements were carried out at the Advanced Light Source beamlines 10 and 12 using 35.5–48 eV photons and at the Stanford Synchrotron Radiation Lightsource (7–22 eV photons) with better than 15 meV energy resolution and overall angular resolution better than 1% of the Brillouin zone. Samples were cleaved and measured at 15 K, in a vacuum maintained below 8×10^{-11} torr. Momentum along the $\hat{z}$ axis is determined using an inner potential of 9.5 eV, consistent with previous photoemission investigations of undoped Bi_2Se_3 (ref. 6). Large single crystals of $Cu_xBi_2Se_3$ were grown using methods described in the Supplementary Information. Surface- and bulk-state band calculations were carried out for comparison with the experimental data, using the linearized augmented plane-wave method implemented in the WIEN2K package[30]. Details of the calculation are identical to those described in ref. 6.

Received 4 June 2010; accepted 3 August 2010; published online 19 September 2010

References

1. Moore, J. E. Topological insulators: The next generation. *Nature Phys.* **5,** 378–380 (2009).
2. Hasan, M. Z. & Kane, C. L. Topological insulators. Preprint at http://arxiv.org/abs/1002.3895 (2010).
3. Fu, L. & Kane, C. L. Topological insulators with inversion symmetry. *Phys. Rev. B* **76,** 045302 (2007).
4. Hsieh, D. *et al.* A topological Dirac insulator in a quantum spin Hall phase. *Nature* **452,** 970–974 (2008).
5. Hsieh, D. *et al.* Observation of unconventional quantum spin textures in topological insulators. *Science* **323,** 919–922 (2009).
6. Xia, Y. *et al.* Observation of a large-gap topological-insulator class with a single Dirac cone on the surface. *Nature Phys.* **5,** 398–402 (2009).
7. Lin, H. *et al.* Single-Dirac-cone topological surface states in the $TlBiSe_2$ class of topological insulators. *Phys. Rev. Lett.* **105,** 036404 (2010).
8. Hsieh, D. *et al.* A tunable topological insulator in the spin helical Dirac transport regime. *Nature* **460,** 1101–1105 (2009).

9. Kitaev, A. *Proc. of the L.D. Landau Memorial Conf. 'Advances in Theoretical Physics', June 22–26* (2008).
10. Volovik, G. E. *The Universe in a Helium Droplet* (Clarendon Press, 2003).
11. Schnyder, A. P. *et al.* Classification of topological insulators and superconductors in three spatial dimensions. *Phys. Rev. B* **78,** 195125 (2008).
12. Fu, L. & Kane, C. L. Superconducting proximity effect and Majorana fermions at the surface of a topological insulator. *Phys. Rev. Lett.* **100,** 096407 (2008).
13. Wilczek, F. Majorana returns. *Nature Phys.* **5,** 614–618 (2009).
14. Bray-Ali, N., Ding, L. & Haas, S. Topological order in paired states of fermions in two-dimensions with breaking of parity and time-reversal symmetries. *Phys. Rev. B* **80,** 180504(R) (2009).
15. Qi, X-L., Hughes, T. L. & Zhang, S-C. Fermi surface topological invariants for time reversal invariant superconductors. *Phys. Rev. B* **81,** 134508 (2010).
16. Santos, L. *et al.* Superconductivity on the surface of topological insulators and in two-dimensional noncentrosymmetric materials. *Phys. Rev. B* **81,** 184502 (2010).
17. Linder, J. *et al.* Unconventional superconductivity on a topological insulator. *Phys. Rev. Lett.* **104,** 067001 (2010).
18. Hosur, P., Ryu, S. & Vishwanath, A. 'Chiral' topological insulators, superconductors and other competing orders in three-dimensions. *Phys. Rev. B* **81,** 045120 (2010).
19. Garate, I. & Franz, M. Inverse spin-galvanic effect in a topological-insulator/ferromagnet interface. *Phys. Rev. Lett.* **104,** 146802 (2010).
20. Fu, L. & Berg, E. Odd-parity topological superconductors: theory and application to $Cu_xBi_2Se_3$. Preprint at http://arxiv.org/abs/0912.3294 (2009).
21. Hasan, M. Z. *et al.* Warping the cone on a topological insulator. *Physics* **2,** 108 (2009).
22. Hor, Y. S. *et al.* Superconductivity in $Cu_xBi_2Se_3$ and its implications for pairing in the undoped topological insulator. *Phys. Rev. Lett.* **104,** 057001 (2010).
23. Hor, Y. S. *et al.* Superconductivity and non-metallicity induced by doping the topological insulators Bi_2Se_3 and Bi_2Te_3. Preprint at http://arxiv.org/abs/1006.0317 (2010).
24. Nayak, C. Exotic matter: Another dimension for anyons. *Nature* **464,** 693–694 (2010).
25. Vasko, A. Amphoteric nature of copper in Bi_2Se_3 crystals. *Appl. Phys.* **5,** 217–221 (1974).
26. Carlson, E. W. *et al.* in *The Physics of Conventional and Unconventional Superconductors* (eds Bennemann, K. H. & Ketterson, J. B.) (Springer-Verlag, 2002).
27. Qian, D. *et al.* Low-lying quasiparticle states and hidden collective charge instabilities in parent cobaltate superconductors. *Phys. Rev. Lett.* **96,** 216405 (2006).
28. Hsieh, D. *et al.* Observation of time-reversal-protected single-Dirac-cone topological-insulator states in Bi_2Te_3 and Sb_2Te_3. *Phys. Rev. Lett.* **103,** 146401 (2009).
29. Lin, H. *et al.* Half-Heusler ternary compounds as new multifunctional experimental platforms for topological quantum phenomena. *Nature Mater.* **9,** 546–549 (2010).
30. Blaha, P. *et al. Computer Code WIEN2K* (Vienna University of Technology, 2001).

Acknowledgements

We acknowledge helpful discussions with L. Fu, A. Kitaev, F.D.M. Haldane and A. Ludwig. The synchrotron X-ray-based measurements and theoretical computations are supported by the Basic Energy Sciences of the US DOE (DE-FG-02-05ER46200, AC03-76SF00098 and DE-FG02-07ER46352). We are grateful for beamline support from S.K. Mo, D. Lu and R. Moore. Materials growth and characterization are supported by NSF/DMR-0819860. M.Z.H. acknowledges additional support from the A.P. Sloan Foundation.

Author contributions

L.A.W. and S-Y.X. contributed equally to the experiment with assistance from Y.X., D.Q. and M.Z.H.; A.V.F. provided beamline assistance; Y.S.H. and R.J.C. provided samples; H.L. and A.B. carried out the theoretical calculations; M.Z.H. was responsible for the overall direction, planning and integration among different research units.

Additional information

The authors declare no competing financial interests. Supplementary information accompanies this paper on www.nature.com/naturephysics. Reprints and permissions information is available online at http://npg.nature.com/reprintsandpermissions. Correspondence and requests for materials should be addressed to M.Z.H.